Scattering Theory of Nonlinear Thermoelectric Transport

David Sánchez[1,2] and Rosa López[1,2]

[1]Institut de Física Interdisciplinària i de Sistemes Complexos IFISC (UIB-CSIC), E-07122 Palma de Mallorca, Spain
[2]Departament de Física, Universitat de les Illes Balears, E-07122 Palma de Mallorca, Spain

(Received 7 August 2012; revised manuscript received 12 December 2012; published 11 January 2013)

We investigate nonlinear transport properties of quantum conductors in response to both electrical and thermal driving forces. Within the scattering approach, we determine the nonequilibrium screening potential of a generic mesoscopic system and find that its response is dictated by particle and entropic injectivities which describe the charge and entropy transfer during transport. We illustrate our model analyzing the voltage and thermal rectification of a resonant tunneling barrier. Importantly, we discuss interaction induced contributions to the thermopower in the presence of large temperature differences.

DOI: 10.1103/PhysRevLett.110.026804 PACS numbers: 73.23.−b, 73.50.Fq, 73.50.Lw, 73.63.Kv

Introduction.—Recent advances in nanoscale thermoelectric materials suggest novel functionalities and highly improved performances [1]. A key ingredient of thermoelectric devices is the Seebeck effect, which depends on the simultaneous existence of thermal and electric driving forces. As a result, energy conversion from waste heat is possible under the conditions of zero net current. The Seebeck coefficient S measures the amount of thermovoltage generated across a conducting sample when a thermal gradient is externally applied. Interestingly, the thermoelectric figure of merit is proportional to S^2. Therefore, it is highly desirable to put forward new routes to increase S. Electron-electron interactions may dramatically enhance S in strongly correlated systems as in magnetically diluted metallic hosts [2] and artificial Kondo impurities [3].

On the other hand, large temperature drops give rise, quite generally, to thermal rectification effects [4]. The possibility to apply sharp thermal gradients seems to be more feasible in nanostructured materials, as recently demonstrated in superlattices with periods spanning a few nanometers [5]. Strikingly enough, a self-consistent theory of nonlinear thermoelectric transport valid for quantum conductors is still lacking. This is the gap we want to fill in this work.

Linear thermoelectric effects within the scattering approach were discussed in Ref. [6]. At the same time, pioneering experiments analyzed the main properties of the thermopower at linear response in quantum point contacts [7] and quantum dots [8]. Subsequent advances have unveiled fluctuating thermopower in chaotic dots [9], large S in Andreev interferometers [10] and thermoelectric anisotropies in multiterminal ballistic microjunctions [11]. The Seebeck coefficient can also help determine the conduction character of a molecular junction [12]. Only recently has a clear observation of thermal rectification effects in mesoscopic systems been possible [13]. Thus, it is natural to ask how phase-coherent current and thermopower are affected in the nonlinear regime of transport.

In the isothermal case, all terminals are held at the same background temperature T. References [14,15] then provide a convenient theoretical framework to include nonequilibrium effects beyond linear response. The theory is based on an expansion around the equilibrium point but, importantly, the nonlinear transport coefficients are complicated functions of the screening response of the conductor out of equilibrium. This purely interaction driven response is described in terms of characteristic potentials that measure how the internal potential counterbalance the ensuing charge pileup due to a voltage shift. Hence, the characteristic potentials depend on the particle injectivity of those carriers originated in the shifted terminal. The role of these particle injectivities is crucial because they determine departures from the Onsager-Casimir symmetry relations [16,17] ubiquitously found in nonlinear transport experiments [18–22]. Here, we show that when the system is perturbed with a temperature shift its response is dictated by entropic injectivities, which quantify the entropy transported in the charge imbalance process. Below, we discuss the role of both particle and entropic injectivities in two conceptually simple but generic problems—the formation of rectifying terms in thermally driven electric currents and the differential Seebeck coefficient beyond linear response.

Theoretical model.—We consider a mesoscopic conductor coupled to multiple terminals $\alpha, \beta, \ldots$ characterized with bias voltages $eV_\alpha = \mu_\alpha - E_F$ (μ_α is the electrochemical potential and E_F the Fermi energy) and temperature shifts $\theta_\alpha = T_\alpha - T$ (T_α is the reservoir temperature). The electronic transport is completely determined by the scattering matrix $s_{\alpha\beta} = s_{\alpha\beta}[E, eU(\vec{r})]$, which, in general, is a function of the carrier energy E and the potential landscape inside the conductor $U(\vec{r})$ [14,15]. In turn, $U(\vec{r})$ is a function of position $\vec{r}$ and the set of voltage and temperature shifts. Defining $A_{\alpha\beta} = \mathrm{Tr}[\delta_{\alpha\beta} - s^\dagger_{\alpha\beta} s_{\alpha\beta}]$, the electrical current is expressed as $I_\alpha = \frac{2e}{h} \sum_\beta \int dE A_{\alpha\beta}(E) f_\beta(E)$ where $f_\beta(E) = 1/\{1 + \exp[(E - E_F - eV_\beta)/k_B T_\beta]\}$ is the Fermi distribution

function in reservoir β. In the weakly nonlinear regime of transport, the dominant terms appear up to second order in an expansion of the electric current in powers of the driving fields V_α and θ_α:

$$I_\alpha = \sum_\beta G_{\alpha\beta} V_\beta + \sum_\beta L_{\alpha\beta}\theta_\beta + \sum_{\beta\gamma} G_{\alpha\beta\gamma} V_\beta V_\gamma + \sum_{\beta\gamma} L_{\alpha\beta\gamma}\theta_\beta\theta_\gamma + 2\sum_{\beta\gamma} M_{\alpha\beta\gamma} V_\beta \theta_\gamma. \quad (1)$$

The electrical and thermoelectric linear conductances are [6] $G_{\alpha\beta} = -(2e^2/h)\int dE A_{\alpha\beta}\partial_E f \simeq (2e^2/h)A_{\alpha\beta}(E_F)$ and $L_{\alpha\beta} = -(2e/hT)\int dE(E-E_F)A_{\alpha\beta}\partial_E f \simeq (2e\pi^2 k_B^2 T/3h)\times \partial_E A_{\alpha\beta}|_{E=E_F}$, respectively, where the approximate expressions correspond to a Sommerfeld expansion to leading order in $k_B T/E_F$. Here, f is the Fermi distribution function when all V_α and θ_α are set to zero. We emphasize that the linear conductances are evaluated at equilibrium and, as a consequence, $G_{\alpha\beta}$ and $L_{\alpha\beta}$ are independent of the screening potential U. The situation is completely different for the nonlinear coefficients. We find

$$G_{\alpha\beta\gamma} = \frac{-e^2}{h}\int dE\left(\frac{\partial A_{\alpha\beta}}{\partial V_\gamma} + \frac{\partial A_{\alpha\gamma}}{\partial V_\beta} + e\delta_{\beta\gamma}\partial_E A_{\alpha\beta}\right)\partial_E f, \quad (2a)$$

$$L_{\alpha\beta\gamma} = \frac{e}{h}\int dE\frac{E_F - E}{T}\left(\frac{\partial A_{\alpha\beta}}{\partial\theta_\gamma} + \frac{\partial A_{\alpha\gamma}}{\partial\theta_\beta} + \delta_{\beta\gamma}\Xi_{\alpha\beta}\right)\partial_E f, \quad (2b)$$

$$M_{\alpha\beta\gamma} = \frac{e^2}{h}\int dE\left(\frac{E_F - E}{eT}\frac{\partial A_{\alpha\gamma}}{\partial V_\beta} - \frac{\partial A_{\alpha\beta}}{\partial\theta_\gamma} - \delta_{\beta\gamma}\Xi_{\alpha\beta}\right)\partial_E f, \quad (2c)$$

where $\Xi_{\alpha\beta} = [(E-E_F)/T]\partial_E A_{\alpha\beta}$. Notably, the nonlinear responses depend on how the scattering matrix changes, through the potential U, in response to a shift in voltage or temperature. Because we are concerned with small changes away from equilibrium, an expansion of U up to first order suffices:

$$U = U_{\rm eq} + \sum_\alpha u_\alpha V_\alpha + \sum_\alpha z_\alpha\theta_\alpha, \quad (3)$$

where $u_\alpha = (\partial U/\partial V_\alpha)_{\rm eq}$ and $z_\alpha = (\partial U/\partial\theta_\alpha)_{\rm eq}$ are characteristic potentials that describe the internal change of the system to a shift of voltage and temperature, respectively, applied to terminal α. In the sequel, we derive the self-consistent procedure to determine the electrostatic potential in the presence of electrical and thermal forces.

The net charge response of the system away from its equilibrium state can be decomposed into two terms, namely, the *bare* charge injected from lead α and the screening charge that builds up in the conductor due to interaction with the injected charges: $q = q_{\rm bare} + q_{\rm scr}$. The contribution to $q_{\rm bare}$ due to a voltage imbalance in lead α is given by the particle injectivity $\nu_\alpha^p(E)$. This is a partial density of states associated with scattering states that describe those carriers originated from lead α [14]. In addition, a shift of temperature in lead α also induces a change in $q_{\rm bare}$. In contrast to the voltage case, however, where every carrier with an energy E contributes positively to $q_{\rm bare}$, in the thermally bias case the contribution of a temperature shift in lead α gives rise to a heat addition or removal depending on whether the carrier energy E is larger or smaller than E_F [23]. This crucial fact must be reflected in the entropic injectivity denoted by ν_α^e:

$$\nu_\alpha^p(E) = \frac{1}{2\pi i}\sum_\beta {\rm Tr}\left[s_{\beta\alpha}^\dagger\frac{ds_{\beta\alpha}}{dE}\right], \quad (4)$$

$$\nu_\alpha^e(E) = \frac{1}{2\pi i}\sum_\beta {\rm Tr}\left[\frac{E-E_F}{T}s_{\beta\alpha}^\dagger\frac{ds_{\beta\alpha}}{dE}\right]. \quad (5)$$

To be concise, we have assumed that the potential is homogeneous (i.e., position independent) within the sample (the extension to inhomogeneous fields is straightforward [15]) and that the WKB approximation applies in order to make the replacement $\delta/\delta U \to -e\partial/\partial E$. We note that the factor $(E-E_F)/T$ represents the entropy transfer associated with adding a single carrier [24]. Then the accumulation or depletion bare charge imbalance due to voltage or to temperature shifts becomes $q_{\rm bare} = e\sum_\alpha(D_\alpha^p eV_\alpha + D_\alpha^e\theta_\alpha)$ where $D_\alpha^p = -\int dE\nu_\alpha^p(E)\partial_E f$, and $D_\alpha^e = -\int dE\nu_\alpha^e(E)\partial_E f$. Next, we obtain the screening charge from the response of the internal potential, $\Delta U = U - U_{\rm eq}$, to changes in the leads' chemical potential and temperature. Within the random phase approximation, one has $q_{\rm scr} = e^2\Pi\Delta U$. Π is the Lindhard function which in the static case (frequency-dependent effects are not considered here) and in the long wavelength limit reads $\Pi = -\sum_\alpha D_\alpha^p = -D$ at $T = 0$ [$D = D(E_F)$ is the sample density of states] [25]. These approximations are excellent for our purpose because (i) if $T \neq 0$ one can simply replace the previous expression with $\Pi = \int dE D(E)\partial_E f$, and (ii) the long wavelength limit amounts to carrier energies well below the tunnel barrier heights that couple the conductor to the external reservoirs. But this is precisely the range of validity of the WKB approximation used to express D^p and D^e in terms of energy derivatives only.

Our set of equations is closed when we relate the out-of-equilibrium net charge with ΔU employing the Poisson equation, $\nabla^2\Delta U = -4\pi q$. We use Eq. (3) and the fact that V_α and θ_α shifts are independent. We then identify a pair of separated equations, $\nabla^2 u_\alpha + 4\pi e^2\Pi u_\alpha = -4\pi e^2 D_\alpha^p$ and $\nabla^2 z_\alpha + 4\pi e^2\Pi z_\alpha = -4\pi e D_\alpha^e$, which become nonlocal in the case of inhomogeneous fields.

The voltage and temperature derivatives, $\partial_{\theta_\gamma}A_{\alpha\beta}$ and $\partial_{V_\gamma}A_{\alpha\beta}$, can be determined once the characteristic potentials are known since $\partial_{\theta_\gamma}A_{\alpha\beta} = z_\gamma\delta A_{\alpha\beta}/\delta U \to -ez_\gamma\partial_E A_{\alpha\beta}$ and $\partial_{V_\gamma}A_{\alpha\beta} = u_\gamma\delta A_{\alpha\beta}/\delta U \to -eu_\gamma\partial_E A_{\alpha\beta}$. Thus, Eq. (2) becomes

$$G_{\alpha\beta\gamma} = \frac{e^3}{h}\int dE[\partial_E A_{\alpha\gamma} u_\beta + \partial_E A_{\alpha\beta}(u_\gamma - \delta_{\beta\gamma})]\partial_E f, \tag{6a}$$

$$L_{\alpha\beta\gamma} = \frac{e^2}{h}\int dE\left[\Xi_{\alpha\gamma} z_\beta + \Xi_{\alpha\beta}\left(z_\gamma - \frac{E-E_F}{eT}\delta_{\beta\gamma}\right)\right]\partial_E f, \tag{6b}$$

$$M_{\alpha\beta\gamma} = \frac{e^2}{h}\int dE[e\partial_E A_{\alpha\beta} z_\gamma + \Xi_{\alpha\gamma} u_\beta - \Xi_{\alpha\beta}\delta_{\beta\gamma}]\partial_E f. \tag{6c}$$

This is our central result. Importantly, Eq. (6) is not only of formal interest but offers clearly practical advantages.

Quantum dot.—As an illustrative application of the formalism exposed above, we now investigate the nonlinear thermoelectric transport properties of a quantum dot when Coulomb interactions are treated within a mean-field approximation. Preliminary observations suggest interesting nonlinear thermoelectric effects in quantum dots [26]. We consider a single level with energy E_d coupled to two reservoirs (1 and 2) via tunnel barriers (see inset of Fig. 1). Thus, the level acquires a broadening given by $\Gamma = \Gamma_1 + \Gamma_2$. The corresponding Breit-Wigner line shape depends, quite generally, on the internal potential U, which is self-consistently calculated through the Poisson equation. The dot charge is then

$$q_d = \frac{e}{\pi}\int dE \frac{\Gamma_1 f_1(E) + \Gamma_2 f_2(E)}{(E - E_d - eU)^2 + \Gamma^2}. \tag{7}$$

We expand Eq. (7) to leading order in V_α, θ_α, and U. We find $\delta q_d = e^2 D_1^p V_1 + e^2 D_2^p V_2 + e D_1^e \theta_1 + e D_2^e \theta_2 - e^2 D U$,

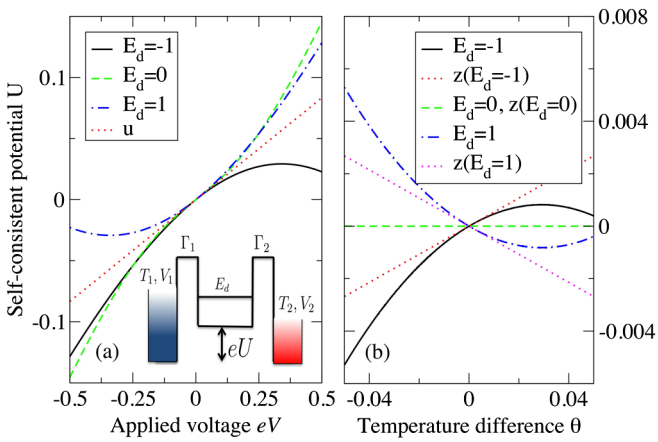

FIG. 1 (color online). Self-consistent screening potential U for a quantum dot system with $V_1 = V/2$, $V_2 = -V/2$ ($E_F = 0$), $T_1 = T + \theta/2$, and $T_2 = T - \theta/2$ (see inset). We take $k_B = e = h = 1$ and $E_F = 0$. (a) U at $\theta = 0$ for $T = 0.01$, $\Gamma_1 = 2\Gamma_2 = 0.2$ and various dot level positions E_d. The dotted line corresponds to the leading-order approximation $U = uV = \eta V/2$ independently of E_d. (b) U at $V = 0$ for $T = 0.05$, $\Gamma_2 = 2\Gamma_1 = 0.2$, and $E_d = \pm 1, 0$. Dotted lines correspond to $U = z\theta$ with the characteristic potential calculated from Eq. (9).

where $\delta q_d = q_d - q_d^e$ denote the charge excess due to voltage and temperature shifts and q_d^e is the equilibrium charge given by Eq. (7) with $f_1 = f_2 = f$. $D_\alpha^p = -\frac{\Gamma_\alpha}{\pi}\int dE \frac{1}{(E-E_d)^2+\Gamma^2}\partial_E f$ and $D_\alpha^e = -\frac{\Gamma_\alpha}{\pi}\int dE \frac{E-E_F}{T} \times \frac{1}{(E-E_d)^2+\Gamma^2}\partial_E f$ are the integrated particle and entropic injectivities of Eqs. (4) and (5) when the Breit-Wigner representation is used.

In a discrete form, the Poisson equation is written in terms of a geometrical capacitance C that electrically connects the dot to an external gate terminal. Accordingly, the charge excess of the dot obeys $\delta q_d = C(U - V_g)$ where V_g is the gate potential. Then,

$$U = \frac{e^2 D_1^p V_1 + e^2 D_2^p V_2 + e D_1^e \theta_1 + e D_2^e \theta_2 + C V_g}{C + e^2 D}, \tag{8}$$

from which the characteristic potentials follow,

$$u_{1(2)} = \frac{e^2 D_{1(2)}^p}{C + e^2 D}, \quad u_g = \frac{C}{C + e^2 D}, \quad z_{1(2)} = \frac{e D_{1(2)}^e}{C + e^2 D}. \tag{9}$$

Rectification effects.—We consider the charge neutral limit ($C = 0$) because it applies to the experimentally relevant case of strong interactions. Moreover, if the dot is symmetrically biased ($V_1 = V/2$, $V_2 = -V/2$, $T_1 = T + \theta/2$, and $T_2 = T - \theta/2$) then $u = \partial U/\partial V = \eta/2$ and $z = \partial U/\partial\theta = (D_1^e - D_2^e)/[2e(D_1^p + D_2^p)]$ to leading order in V and θ with $\eta = (\Gamma_1 - \Gamma_2)/\Gamma$ the tunneling asymmetry [16]. In Fig. 1 we show the exact dot potential obtained from a numerical calculation of Eq. (7) compared to its approximate value [Eq. (8)]. We distinguish between the isothermal case [$\theta = 0$, Fig. 1(a)] and the isoelectric case [$V = 0$, Fig. 1(b)]. In the former, the self-consistent potential is plotted for three values of the dot level $E_d = \pm 1, 0$. The curves for the exact U agree with approximation $U = uV$ at low V, as expected. In the strongly nonlinear regime and for $E_d = \pm 1$, higher-order terms (V^2 or higher) make U depart from its linearity. We recall that linear responses depend on $U_{\rm eq}$ only and they are insensitive to the variation of U with V. Only the nonlinear current allows us to explore this regime. Interestingly, at resonance ($E_d = 0$) the contributions to U from even powers in V are absent. In the isoelectric case [Fig. 1(b)], we present U in response to a thermal shift for $E_d = \pm 1, 0$. Particularly interesting is the particle-hole symmetry case $E_d = 0$ for which U vanishes to all θ powers. We also compare the full calculation with the leading-order approximation $U = z\theta$. Notice that contrary to the isoelectric case z depends on E_d. The agreement is quite reasonable at low-temperature shifts.

The evolution of the current for an electrically and thermally driven quantum dot is shown in Fig. 2(a) and Fig. 2(b), respectively, for fixed $E_d = 1$. For $\theta = 0$ the current first follows Ohm's law at low V and then, at higher voltages, acquires a V^2 dependence leading to rectification effects. The I-V curves can be approximated up to V^2 with

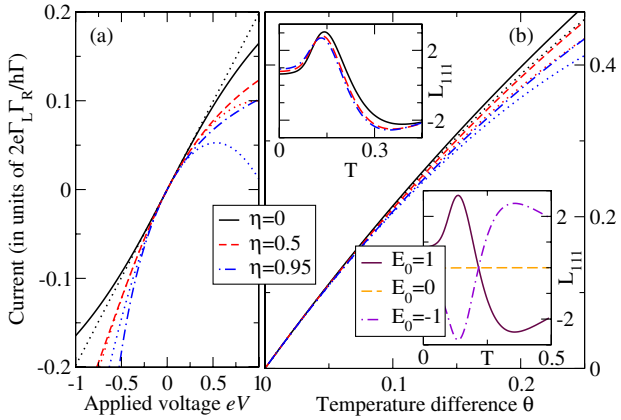

FIG. 2 (color online). Electrical current for a quantum dot system with $V_1 = V/2$, $V_2 = -V/2$, $T_1 = T + \theta$, and $T_2 = T$ for $\Gamma = 0.2$ and three different values of the tunneling asymmetry η. (a) I-V characteristics for $\theta = 0$ and $T = 0.01$ along with the leading-order nonlinearity $I \simeq G_{11}V + G_{111}V^2$. The latter correspond to the dotted lines. (b) I-θ characteristics for $V = 0$ and $T = 0.5$. Dotted lines correspond to $I \simeq L_{11}\theta + L_{111}\theta^2$. Upper inset: L_{111} versus T as a function of η for $E_d = 1$. Lower inset: L_{111} for $E_d = \pm 1$, 0 and $\eta = 0$.

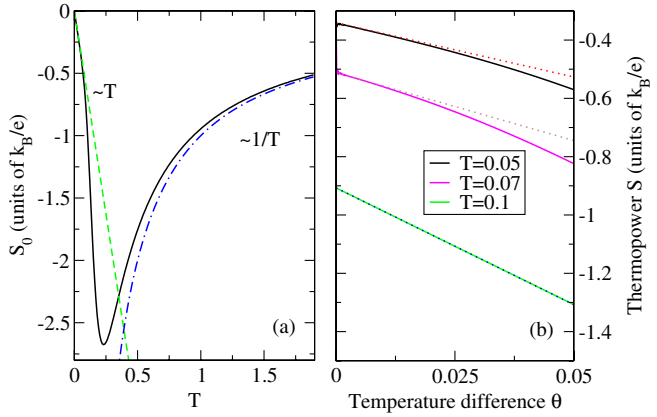

FIG. 3 (color online). (a) Linear-response thermopower S_0 for a symmetrically voltage biased dot and one heated contact ($\theta_1 = \theta$ and $\theta_2 = 0$) at $E_d = 1$. Low and high temperature limits of S_0 are explicitly shown. (b) Thermopower S beyond linear response for three different background temperature values. We show with dotted lines the leading-order expansion $S \simeq S_0 + S_1\theta$ calculated from the sensitivity given by Eq. (11).

$I = G_{11}V + G_{111}V^2 + \mathcal{O}(V^3)$ where the leading-order nonlinearity in the Sommerfeld approximation, $G_{111} = \frac{e^3}{h}\partial_E A_{11}|_{E=E_F}(1 - 2u_1)$, depends on the internal potential response. The I-V curves in Fig. 2(a) correspond to three values of η and show good agreement with the second-order expansion except for very high voltages. In Fig. 2(b) we show I driven by a temperature shift for $V = 0$. We compare the full I-θ characteristics for different η values with the second-order expansion, $I = L_{11}\theta + L_{111}\theta^2 + \mathcal{O}(\theta^3)$, where the thermal rectification term is

$$L_{111} = \frac{e\pi^2 k_B^2}{3h}(\partial_E A_{11}|_{E=E_F} - 2ez_1 T\partial_E^2 A_{11}|_{E=E_F}), \qquad (10)$$

to leading order in the Sommerfeld approximation. First, I grows linearly with θ and then higher orders in θ become relevant above a threshold where L_{111} is large enough. We plot L_{111} in Fig. 2(b) (upper inset) and find a nonmonotonic behavior with the background temperature T. We also show Fig. 2(b) (lower inset) the dependence of L_{111} for various level positions and $\eta = 0$. Interestingly, in the particle-hole symmetry point L_{111} vanishes identically (like L_{11}) whereas for $E_d = \pm 1$, L_{111} presents an opposite behavior as a function of T. It also follows from Eq. (10) that for $T = 0$ L_{111} is generally nonzero unlike L_{11}.

Thermopower.—The thermopower S yields the voltage generated across the sample in response to an applied thermal bias at vanishing current condition. In the linear transport regime and for a two-terminal conductor, the Seebeck coefficient is $S_0 = V/\theta|_{I=0} = -L_{11}/G_{11}$. This expression is correct in the limit $\theta \to 0$. At low temperatures, it can be approximated to the Mott formula $S_0 \simeq -(\pi^2 k_B^2 T/3e)\partial_E \ln A_{11}|_{E=E_F} \propto T$ whereas for high T we find $S_0 \simeq (E_F - E_d)/eT \propto T^{-1}$ in the limit $\Gamma \ll k_B T$. In Fig. 3(a) we numerically calculate S_0 for an electrically biased quantum dot ($V_1 = -V_2 = -V/2$) when only one reservoir is heated ($\theta_1 = \theta$ and $\theta_2 = 0$). Our numerical simulations reproduce the analytical T dependence both at low temperature (Mott relation) and at high temperature (infinitely narrow resonance). More interesing are the θ corrections to S when θ is not small. Then, we can expand $S = S_0 + S_1\theta + \mathcal{O}(\theta^2)$ where the S_1 is the thermopower sensitivity, which measures the deviations of S from a constant value. Importantly, a measurement of the differential thermopower $dS/d\theta$ gives precisely S_1 to leading order in θ. Specializing Eq. (1) to the two-terminal case and setting $I = 0$ we find

$$S_1 = -\frac{1}{G_{11}^3}[G_{111}L_{11}^2 + L_{111}G_{11}^2 + G_{11}L_{11}(M_{121} - M_{111})], \qquad (11)$$

valid when a single lead is heated. Inserting Eq. (2) in Eq. (11), we compare the sensitivity with an exact calculation of S for a quantum dot as above. We observe in Fig. 3(a) that excellent agreement is found for low θ and that departures depend on the particular value of T. It is also noteworthy that in the low-T limit the second term in brackets of Eq. (11) dominates because $L_{11} \propto T^2$ and $L_{11}(M_{121} - M_{111}) \propto T^2$ within a Sommerfeld expansion. Then, according to Eq. (10) a low-temperature measurement of the thermopower sensitivity would provide information on the renormalization of the dot level due to a temperature gradient.

Conclusions.—We have presented a general nonlinear scattering theory for mesoscopic conductors that are driven by electrical and thermal gradients. In the weakly nonlinear regime, screening effects arise in response to charge

pile-up due to voltage or temperature differences. Importantly, the transmission probability becomes a function of the thermal gradient. We have found that the screening response can be described in terms of both particle and entropic injectivities. We have illustrated our theory with an application to a two-terminal quantum dot setup, evaluating the current-voltage and current-temperature characteristics. Importantly, we have discussed thermopower sensitivity in the nonlinear regime of transport. Our results are relevant in view of recent advances in thermoelectrics at the nanoscale.

We thank M. Büttiker and H. Linke for useful suggestions. This work is supported by MINECO Grant No. FIS2011-23526.

[1] *Thermoelectrics Handbook. Macro to Nano*, edited by D. M. Rowe (CRC Press, Boca Raton, FL, 2006).
[2] N. E. Bickers, D. L. Cox, and J. W. Wilkins, Phys. Rev. Lett. **54**, 230 (1985).
[3] T. A. Costi and V. Zlatić, Phys. Rev. B **81**, 235127 (2010).
[4] M. Terraneo, M. Peyrard, and G. Casati, Phys. Rev. Lett. **88**, 094302 (2002).
[5] R. Venkatasubramanian, E. Siivola, T. Colpitts, and B. O'Quinn, Nature (London) **413**, 597 (2001).
[6] P. N. Butcher, J. Phys. Condens. Matter **2**, 4869 (1990).
[7] L. W. Molenkamp, Th. Gravier, H. van Houten, O. J. A. Buijk, M. A. A. Mabesoone, and C. T. Foxon, Phys. Rev. Lett. **68**, 3765 (1992).
[8] A. A. M. Staring, L. W. Molenkamp, B. W. Alphenaar, H. van Houten, O. J. A. Buyk, M. A. A. Mabesoone, C. W. J. Beenakker, and C. T. Foxon, Europhys. Lett. **22**, 57 (1993).
[9] S. F. Godijn, S. Möller, H. Buhmann, L. W. Molenkamp, and S. A. van Langen, Phys. Rev. Lett. **82**, 2927 (1999).
[10] J. Eom, C.-J. Chien, and V. Chandrasekhar, Phys. Rev. Lett. **81**, 437 (1998).
[11] J. Matthews, D. Sánchez, M. Larsson, and H. Linke, Phys. Rev. B **85**, 205309 (2012).
[12] P. Reddy, S.-Y. Jang, R. A. Segalman, and A. Majumdar, Science **315**, 1568 (2007).
[13] R. Scheibner, M. König, D. Reuter, A. D. Wieck, C. Gould, H. Buhman, and L. W. Molenkamp, New J. Phys. **10**, 083016 (2008).
[14] M. Büttiker, J. Phys. Condens. Matter **5**, 9361 (1993).
[15] T. Christen and M. Büttiker, Europhys. Lett. **35**, 523 (1996).
[16] D. Sánchez and M. Büttiker, Phys. Rev. Lett. **93**, 106802 (2004); Phys. Rev. B **72**, 201308 (2005).
[17] B. Spivak and A. Zyuzin, Phys. Rev. Lett. **93**, 226801 (2004).
[18] C. A. Marlow, R. P. Taylor, M. Fairbanks, I. Shorubalko, and H. Linke, Phys. Rev. Lett. **96**, 116801 (2006).
[19] R. Leturcq, D. Sánchez, G. Götz, T. Ihn, K. Ensslin, D. C. Driscoll, and A. C. Gossard, Phys. Rev. Lett. **96**, 126801 (2006).
[20] D. M. Zumbühl, C. M. Marcus, M. P. Hanson, and A. C. Gossard, Phys. Rev. Lett. **96**, 206802 (2006).
[21] L. Angers, E. Zakka-Bajjani, R. Deblock, S. Guéron, H. Bouchiat, A. Cavanna, U. Gennser, and M. Polianksi, Phys. Rev. B **75**, 115309 (2007).
[22] D. Hartmann, L. Worschech, and A. Forchel, Phys. Rev. B **78**, 113306 (2008).
[23] T. E. Humphrey, R. Newbury, R. P. Taylor, and H. Linke, Phys. Rev. Lett. **89**, 116801 (2002).
[24] D. Emin, in *Thermoelectrics Handbook. Macro to Nano*, edited by D. M. Rowe (CRC Press, Boca Raton, FL, 2006).
[25] H. Smith, Phys. Scr. **28**, 287 (1983).
[26] S. F. Svensson, E. A. Hoffmann, N. Nakpathomkun, and H. Linke (unpublished).